

# Influence of the Bilayer Composition on the Binding and Membrane Disrupting Effect of Polybia-MP1, an Antimicrobial Mastoparan Peptide with Leukemic T-Lymphocyte Cell Selectivity

Marcia Perez dos Santos Cabrera,<sup>\*,†</sup> Manoel Arcisio-Miranda,<sup>\*,§</sup> Renata Gorjão,<sup>||</sup> Natália Bueno Leite,<sup>‡</sup> Bibiana Monson de Souza,<sup>†</sup> Rui Curi,<sup>⊥</sup> Joaquim Procopio,<sup>⊥</sup> João Ruggiero Neto,<sup>‡</sup> and Mario Sérgio Palma<sup>†</sup>

<sup>†</sup>UNESP-São Paulo State University, Center of Studies of Social Insects, Institute of Biosciences, 13506-900 Rio Claro, SP, Brazil

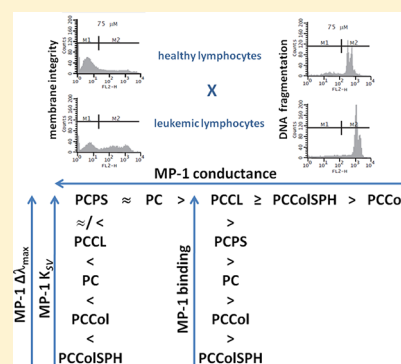
<sup>‡</sup>UNESP-São Paulo State University, Department of Physics, IBILCE, 15054-000 São José do Rio Preto, SP, Brazil

<sup>§</sup>UNIFESP-Universidade Federal de São Paulo, Department of Biophysics, 04923-062 São Paulo, SP, Brazil

<sup>||</sup>Cruzeiro do Sul University, Institute of Sciences of Physical Education and Sports, Post-Graduate Program in Human Movement Science, 01506-000 São Paulo, SP, Brazil

<sup>⊥</sup>USP-University of São Paulo, Department of Physiology and Biophysics, Biomedical Sciences Institute, 05508-900 São Paulo, SP, Brazil

**ABSTRACT:** This study shows that MP-1, a peptide from the venom of the *Polybia paulista* wasp, is more toxic to human leukemic T-lymphocytes than to human primary lymphocytes. By using model membranes and electrophysiology measurements to investigate the molecular mechanisms underlying this selective action, the porelike activity of MP-1 was identified with several bilayer compositions. The highest average conductance was found in bilayers formed by phosphatidylcholine or a mixture of phosphatidylcholine and phosphatidylserine (70:30). The presence of cholesterol or cardiolipin substantially decreases the MP-1 pore activity, suggesting that the membrane fluidity influences the mechanism of selective toxicity. The determination of partition coefficients from the anisotropy of Trp indicated higher coefficients for the anionic bilayers. The partition coefficients were found to be 1 order of magnitude smaller when the bilayers contain cholesterol or a mixture of cholesterol and sphingomyelin. The blue shift fluorescence, anisotropy values, and Stern–Volmer constants are indications of a deeper penetration of MP-1 into anionic bilayers than into zwitterionic bilayers. Our results indicate that MP-1 prefers to target leukemic cell membranes, and its toxicity is probably related to the induction of necrosis and not to DNA fragmentation. This mode of action can be interpreted considering a number of bilayer properties like fluidity, lipid charge, and domain formation. Cholesterol-containing bilayers are less fluid and less charged and have a tendency to form domains. In comparison to healthy cells, leukemic T-lymphocyte membranes are deprived of this lipid, resulting in decreased peptide binding and lower conductance. We showed that the higher content of anionic lipids increases the level of binding of the peptide to bilayers. Additionally, the absence of cholesterol resulted in enhanced pore activity. These findings may drive the selective toxicity of MP-1 to Jurkat cells.



Hymenoptera (bees, wasps, and ants) venoms are a rich source of peptides that exhibit a wide spectrum of biological activities relevant for the development of new drugs, such as cytolytic, antimicrobial, hemolytic, antiparasitic, and tumoricidal drugs.<sup>1–3</sup> Mastoparan peptides from Vespidae venoms have been studied over the past 30 years.<sup>4,5</sup> They are polycationic linear tetradecapeptides that generally have an amidated C-terminus and assume an amphipathic  $\alpha$ -helical structure in the presence of lipid bilayers or their mimetics. In addition, their relatively short chain length represents an advantage when considering the ease of mass production.

Polybia-MP1 (IDWKLLDAAKQIL) is one of the mastoparan peptides found in the venom of the social wasp, *Polybia paulista*.<sup>6,7</sup> It is nonhemolytic to rat erythrocytes, produces mild mast cell degranulation, presents chemotactic activity for

polymorphonuclear leukocytes, and shows potent antimicrobial activity against Gram-positive and Gram-negative bacteria.<sup>6</sup> With 14 amino acid residues and a net charge of +2, Polybia-MP1 exhibits preferential interaction with anionic lipid vesicles over the zwitterionic ones, which is further impaired by the presence of cholesterol.<sup>8</sup> Antimicrobial peptides are usually rich in hydrophobic and basic amino acids, but Polybia-MP1 also contains a considerable amount of acidic and polar residues. Comparing the structural differences between Polybia-MP1 and Mastoparan X, which does not show such selectivity, we

**Received:** October 20, 2011

**Revised:** May 14, 2012

**Published:** May 25, 2012

suggested that the hydrophilicity and the equilibrium of electrostatic interactions may be involved in the absence of hemolytic activity.<sup>8</sup> Thus, considering its interesting biological profile, an improved understanding of interaction of Polybia-MP1 with biological and model membranes would be of potential benefit.

It was recently verified that Polybia-MP1 also presents antitumor effects on prostate and bladder cancer.<sup>3</sup> It is effective against multidrug resistant leukemic cells,<sup>9</sup> and its tumoricidal activity was also confirmed *in vivo*.<sup>10</sup> The basis for its selective toxicity has been attributed to the presence of abnormally high contents of phosphatidylserine in the outer leaflet of the membrane of tumor cells, which is not usually found in healthy cells.<sup>9</sup> However, the antitumor activity of Polybia-MP1 was drastically reduced when a Pro residue replaced the amino acid at position 7, 8, or 9.<sup>3</sup> These substitutions affect the original helical structure and the electrostatic balance and increase the level of hydrophilic character of the peptide (Pro7 and Pro9), which may explain the decrease in the affinity of peptide analogues for lipid bilayers. Together, these findings may be an indication of various mechanisms of selectivity, ranging from those based on preferential binding of the peptide to anionic bilayers to others suggesting a structurally related mechanism.

Considering that the selective mode of action of Polybia-MP1 is still unclear, we focused on the influence of the membrane structure and some of its lipid constituents on its activity. First, we evaluated its toxic effects on human leukemic T-lymphocytes (Jurkat cells) compared to primary lymphocytes by flow cytometry. Afterward, the lipid association of Polybia-MP1 was studied using model membranes made of lipids that are ubiquitous to the membranes of tumor and/or mammalian cells in experiments examining porelike activity on planar bilayers. Additionally, these model membranes were used in experiments involving Trp fluorescence spectroscopy, dynamic light scattering, and  $\zeta$  potential measurements on large unilamellar vesicles (LUVs). We have shown in this study that MP1 is cytotoxic to Jurkat cells by a mechanism that targets the cell membrane. This mechanism is independent of DNA fragmentation and appears to be correlated with the formation of pores in the membrane of these cells, and possibly enhanced by the lower level of cholesterol.

## EXPERIMENTAL PROCEDURES

**Materials.** Avanti Polar Lipids (Alabaster, AL) supplied the phospholipids egg *L*- $\alpha$ -phosphatidylcholine (PC) and 1,2-diphytanoyl-*sn*-glycero-3-phosphocholine (DPhPC), and Sigma-Aldrich Co. (St. Louis, MO) supplied cholesterol (Col), bovine brain sphingomyelin (SPH), bovine heart cardiolipin (CL), and bovine brain *L*- $\alpha$ -phosphatidyl-L-serine (PS). All materials were used as supplied. Lipid stock solutions were prepared in chloroform. Homogeneous films of lipids or lipid mixtures, made free of traces of solvent, were obtained at the following molar ratios: 100% PC (named PC), 80:20 PC:cholesterol (named PCCol), 50:20:30 PC:Chol:sphingomyelin (named PCColSPH), 70:30 PC:CL (named PCCL), and 70:30 PC:PS (named PCPS). Other chemicals were of high-quality analytical grade. PBS was used in tumoricidal activity experiments. PBS, 10 mM Tris-HCl, 1 mM Na<sub>2</sub>EDTA, and 150 mM NaCl (pH 7.5) were used for fluorescence spectroscopy and  $\zeta$  potential experiments, and 10 mM Tris-HCl and 150 mM KCl (pH 7.5) were used for planar bilayers experiments, in which PC was substituted with DPhPC at the same molar concentration.

**Peptide Synthesis, Purification, and Mass Spectrometry Analyses.** Polybia-MP1 was synthesized, as described by De Souza et al.,<sup>6</sup> by stepwise manual solid-phase synthesis using the *N*-9-fluorophenylmethoxycarbonyl (Fmoc) strategy. The crude product was purified by reverse-phase high-performance liquid chromatography (HPLC), and the homogeneity and sequence were accessed by analytical HPLC and mass spectrometry (ESI-MS). Samples were analyzed on a triple quadrupole mass spectrometer, model QUATTRO II, equipped with a standard electrospray (ESI) probe (Micro-mass), adjusted to a rate of  $\sim 250$   $\mu$ L/min. The source temperature was maintained at 80 °C and the needle voltage at 3.6 kV, applying a drying gas flow (nitrogen) of 200 L/h and a nebulizer gas flow of 20 L/h. The mass spectrometer was calibrated with intact horse heart myoglobin and its typical cone voltage-induced fragments. The molecular mass was determined by ESI-MS, adjusting the mass spectrometer to give a peak width at half-height of 1 mass unit. The cone sample to skimmer lens voltage was set to 38 V, controlling the transfer of ions to the mass analyzer. Approximately 50 pmol (10  $\mu$ L) of each sample was injected into the electrospray transport solvent. The ESI spectra were recorded in multichannel acquisition mode. The mass spectrometer data acquisition and treatment system was equipped with MassLynx (Micro-mass) software for handling spectra.

Approximately 100  $\mu$ M Polybia-MP1 stock solutions were prepared in quartz bidistilled water and refrigerated. The final concentration was checked spectrophotometrically using a tryptophan molar absorptivity of 5580 M<sup>-1</sup> cm<sup>-1</sup>.

**Selective Tumoricidal Activity on Human Leukemic Cells versus Normal Lymphocytes.** The study was approved by the Ethical Committee of the Institute of Biomedical Sciences, University of São Paulo. The human blood for lymphocyte isolation was obtained from the Blood Bank of the Federal University of São Paulo. The blood was considered healthy after a routine laboratory analysis.

Jurkat cells were obtained from the Dunn School of Pathology (University of Oxford, Oxford, England). The cells were cultured in RPMI 1640 medium supplemented with 10% fetal bovine serum. This medium was supplemented with glutamine (2 mM), HEPES (20 mM), streptomycin (10000 mg/mL), penicillin (10000 IU/mL), and sodium bicarbonate (24 mM). Cells were grown in 25 mL flasks containing  $1-2 \times 10^6$  cells/mL. The cells were kept in a humidified atmosphere, at 37 °C, containing 5% CO<sub>2</sub>.

**Isolation of Peripheral Blood Lymphocytes.** Peripheral blood lymphocytes were obtained as previously described.<sup>11</sup> Blood was diluted in phosphate-buffered saline (PBS) (1:1), and this suspension was layered on Histopaque-1077 (Sigma Chemical Co.) and centrifuged for 30 min at 400g and room temperature. Peripheral blood mononuclear cells (PBMC; a mixture of monocytes and lymphocytes) were collected from the interphase, lysed with 150 mM NH<sub>4</sub>Cl, 10 mM NaHCO<sub>3</sub>, and 0.1 mM EDTA (pH 7.4), and washed once with PBS. The PBMC were maintained in RPMI 1640 medium for 60 min to allow the adherence of monocytes to the plates, producing a pure lymphocyte preparation ( $\sim 98\%$ ). Lymphocytes were cultured under the same conditions described for Jurkat cells for 24 h before the beginning of the treatment with Polybia-MP1.

**Determination of Cell Membrane Integrity.** Lymphocytes and Jurkat cells were cultured at a density of  $1 \times 10^6$  cells/mL in 24-well plates. Cells were cultured in the absence

and presence of increasing MP-1 concentrations in the range of 25–100  $\mu\text{M}$ , for a period of 24 h. The plates were incubated in a humidified atmosphere of 5%  $\text{CO}_2$  and 95% air, at 37  $^\circ\text{C}$ . After this period, cells were centrifuged at 400g for 15 min at 4  $^\circ\text{C}$ , and the pellet obtained was resuspended in 500  $\mu\text{L}$  of PBS. Afterward, 50  $\mu\text{L}$  of a propidium iodide solution (50 mg/mL in PBS) was added, and the cells were analyzed using a FACSCalibur flow cytometer (Becton Dickinson, San Juan, CA). Fluorescence was measured using the FL2 channel (orange-red fluorescence, 585/42 nm). Ten thousand events were analyzed per experiment. Cells with propidium iodide fluorescence were then evaluated by using the Cell Quest software (Becton Dickinson).

**DNA Staining Using Propidium Iodide.** DNA fragmentation was analyzed by flow cytometry after DNA staining with propidium iodide according to the method described by Nicoletti et al.<sup>12</sup> The presence of Triton in the solution permeabilizes the cell membranes, which promptly incorporate the dye into DNA. Briefly, after incubation with Polybia-MP1 at different concentrations for 24 h, the cells were centrifuged at 400g for 15 min at 4  $^\circ\text{C}$ . The pellet was gently resuspended in 300  $\mu\text{L}$  of a hypotonic solution containing 50 mg/mL propidium iodide, 0.1% sodium citrate, and 0.1% Triton X-100. The cells were then incubated for 1 h at room temperature. Fluorescence was measured and analyzed as described above.

**Statistical Analysis.** Results are presented as means  $\pm$  the standard error of the mean (SEM) of four determinations. Comparisons between groups were performed by analysis of variance (ANOVA). Significant differences were assessed by using the Tukey–Kramer's test (GraphPad Prism, version 5.00 for Windows, GraphPad Software, San Diego, CA). The level of significance was set for  $p < 0.05$ .

**Planar Lipid Bilayer Preparation, Electrophysiology Measurements, and Analysis.** To investigate the basis for the cell selectivity exhibited by MP-1, bilayers composed of ubiquitous phospholipids, which are found in normal mammalian membranes, were used to access the peptide's lytic activity under the most possibly similar physiological conditions. Planar lipid bilayers were formed from the dissolution in *n*-decane of the previously formed phospholipid films at 25 mg/mL (20 mg/mL for PCCol, PCColSPH, and PCCL), according to the original method of Mueller et al.<sup>13</sup> A glass cylindrical cup having a 0.2–0.5 mm hole is coupled to an acrylic chamber; the cup separated two compartments filled with 5 mL of buffer each, designated cis (front chamber, held at ground) and trans (rear chamber, connected to the measuring probe of the amplifier). Electrical access to the baths was through a pair of Ag/AgCl electrodes. Optical reflectance, electrical resistance, and capacitance indicated the formation of planar lipid bilayers. Aliquots of the peptide stock solution were added to the cis compartment and stirred for 3 min using a stream of air obliquely directed over the bath surface. After equilibration for a few minutes, a –50 mV potential was applied to the trans compartment to monitor the initial channel activity. Afterward, the trans side was clamped to a range of potentials and single-channel activity was recorded. The transmembrane current ( $I_m$ ), under different clamping potentials ( $V_{\text{clamp}}$ ), was monitored using a patch-clamp amplifier (Dagan 8900) set into voltage-clamp mode. The membrane conductance ( $G_m$ ) was obtained as  $G_m = I_m/V_{\text{clamp}}$ . Data were acquired using Axotape version 2.0.2 and analyzed with Clampfit version 10.2

(Molecular Devices) and Prism version 4 (GraphPad Software).

**Preparation of Vesicles.** Large unilamellar vesicles (LUVs) were prepared as previously described.<sup>14</sup> Briefly, volumes of <1 mL of LUVs (~10 mM phospholipids) were prepared by the hydration of the lipid films at room temperature or 50  $^\circ\text{C}$  (for mixtures containing cholesterol and/or sphingomyelin) followed by extrusion through polycarbonate membranes (six times through a 400 nm pore and then 11 times through a 100 nm pore), using an Avanti mini-extruder. LUVs were used within 48 h of preparation, refrigerated, and protected from light.

**Steady-State Fluorescence Spectroscopy.** To determine the apparent binding constants and to access the differences in the membrane localization and environment of MP-1 molecules, influenced by the lipid composition of the LUVs, we conducted fluorescence experiments with an ISS (Urbana, IL) PC1 spectrofluorometer. Spectra or single-point measures were recorded with an increment of 1 nm, averaging three to five scans; excitation and emission bandwidths were set to 2 nm, and the temperature was held at 25  $^\circ\text{C}$  with a water circulating bath.

**Fluorescence Spectra.** Increasing aliquots of a vesicle suspension were added to a 5  $\mu\text{M}$  peptide solution in Tris-HCl buffer (pH 7.5) in UV-transparent 220 nm disposable cuvettes (Sarsted Nümbrecht, Germany) to complete the 400  $\mu\text{L}$  sample preparation. Each peptide/vesicle suspension was equilibrated over 30 min, at 25  $^\circ\text{C}$ . The binding of MP-1 to LUVs was followed by the changes in tryptophan emission fluorescence spectra, which were recorded from 305 to 450 nm, with Trp residue excitation set to 280 nm. Correction for scattering artifacts was conducted in two ways, by subtraction of spectra obtained for each lipid concentration from the peptide blank<sup>15</sup> and by using polarizing filters in the excitation and emission pathways set at 90 $^\circ$  and 0 $^\circ$ , respectively.<sup>16</sup> Blue shifts ( $\Delta\lambda_{\text{max}}$ ) were calculated as the differences in the wavelength maxima in emission spectra of the peptide acquired in the presence or absence of vesicles. The standard deviation for the blue shift was 1 nm.

**Trp Fluorescence Emission Anisotropy.** With the excitation and emission set at 285 and 365 nm, respectively, and using Glan-Thompson polarizers, Trp emission anisotropy was determined from the parallel and perpendicular components of the emission, with samples prepared as indicated for the acquisition of Trp emission spectra. Fluorescence anisotropies ( $r$ ) were calculated using the equation  $r = (F^{\parallel} - GF^{\perp}) / (F^{\parallel} + 2GF^{\perp})$ , where  $F^{\parallel}$  is the fluorescence emission intensity parallel to the excitation plane,  $F^{\perp}$  is the normal component to the same plane, and  $G$  is the instrumental factor.<sup>17,18</sup> The partition coefficient,  $K_p$ , can be obtained through the fitting of the plot of the mean anisotropy versus an increasing lipid concentration ( $[L]$ )

$$r = \{r_w[(\gamma_L[L])^{-1} - 1] + r_L K_p \epsilon_L \phi_L / (\epsilon_w \phi_w)\} / (\gamma_L[L])^{-1} - 1 + K_p \epsilon_L \phi_L / (\epsilon_w \phi_w)]$$

and the molar fraction of bound peptide molecules,  $X_B$

$$X_B = \frac{K_p \gamma_L C_L}{1 + K_p \gamma_L C_L}$$



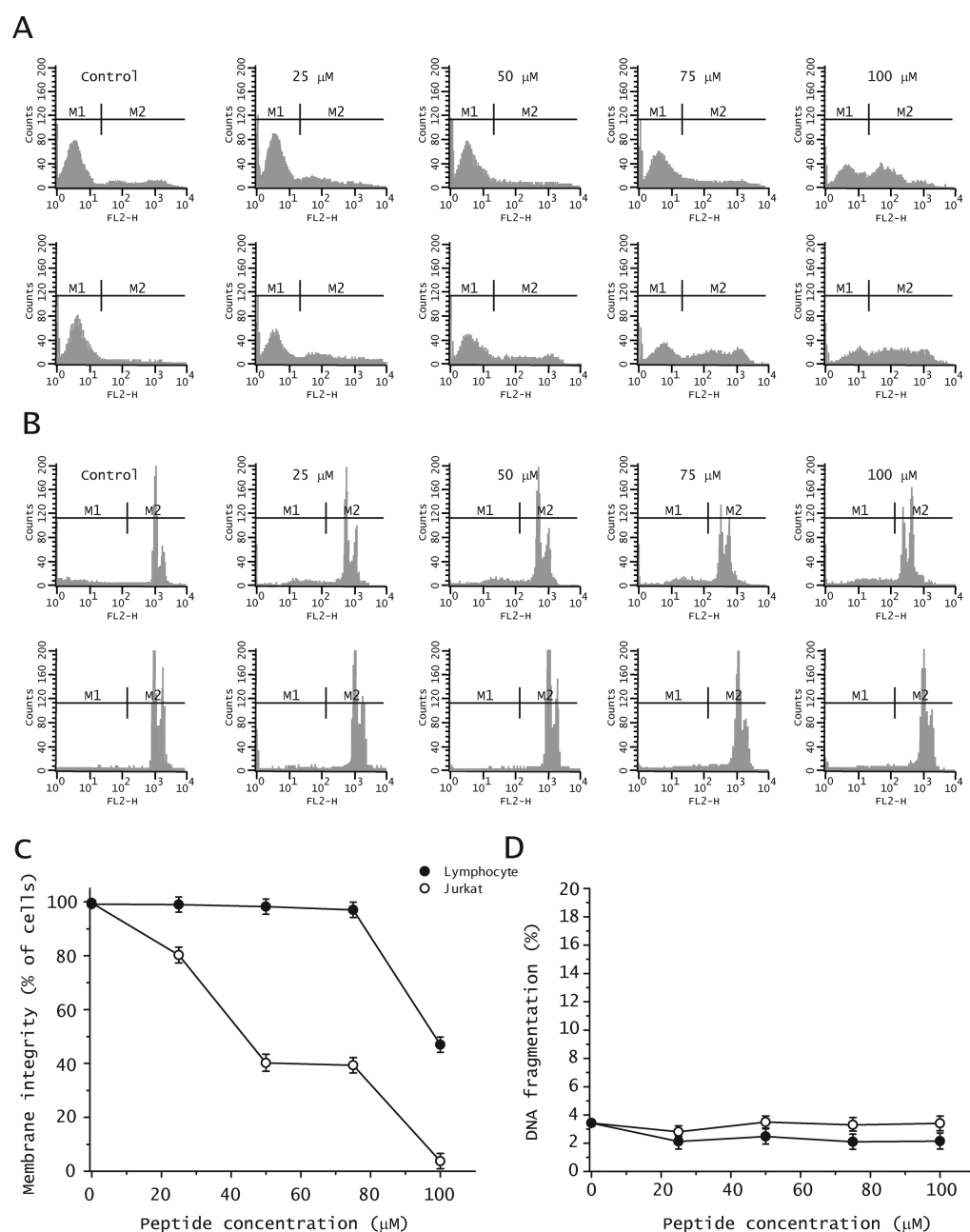


**Figure 1.** Toxicity of MP-1 to human lymphocytes and leukemic T cells. Representative histograms obtained by flow cytometry showing the effects of increasing MP-1 concentrations on (A) membrane integrity and (B) DNA fragmentation in primary lymphocytes (top row) and Jurkat cells (bottom row). In panel A, M1 refers to the cell population showing intact membranes and M2 refers to the population with broken membranes. In panel B, M1 refers to the cell population showing fragmented DNA and M2 to the population with intact DNA. (C and D) Dose–response curves for (C) the percentage of cells showing membrane integrity and (D) the percentage of cells showing DNA fragmentation. Fluorescence was measured in the FL2 channel (orange-red fluorescence, 585 nm, 42 nm). Ten thousand events were analyzed per experiment. The values are presented as means  $\pm$  SEM of four determinations. Comparisons between groups were performed by analysis of variance (ANOVA). The level of significance was set for  $p < 0.05$ .

where  $\gamma_i$  is the lipid molar volume,  $\phi_i$  is the fluorescence quantum yield, and  $\epsilon_i$  is the molar absorption ( $i = W$ , water, and  $i = L$ , lipid phases).<sup>19</sup>

**Quenching of Trp Fluorescence Emission by Acrylamide.** Samples containing 5  $\mu$ M peptide in Tris-HCl buffer (pH 7.5) were prepared in a quartz cell with a path length of 10 mm. Trp fluorescence emission spectra were recorded in the presence and absence of 500  $\mu$ M phospholipid vesicles from 315 to 450 nm (excitation set at 285 nm), after the addition of successive aliquots of a 2.8 M acrylamide solution. The

acrylamide solution was added under agitation with a magnetic stirring bar. Light scattering was minimized by using polarizing filters in the excitation and emission pathways set at 90° and 0°, respectively.<sup>16</sup> Maximal fluorescence intensity data are plotted as  $F_0/F = 1 + K_{SV}(Q)$ , where  $F_0$  and  $F$  are the fluorescence intensities in the absence and presence of the quencher (Q), respectively.  $K_{SV}$  accounts for the concentration of peptide both free in the solvent and bound to the bilayer surface.

**ζ Potential Determination and Dynamic Light Scattering (DLS).** The binding of Polybia-MP1 was first

assessed through the changes in the  $\zeta$  potential of the vesicles, determined in the samples where size distribution was coevaluated by DLS, with a Nano Zetasizer ZS90 (Malvern Instruments, Worcestershire, U.K.), which uses wide angle ( $90^\circ$ ) laser Doppler velocimetry to measure the electrophoretic mobility. The  $\zeta$  potential was calculated by applying the Smoluchowski approximation:  $\zeta = \eta\mu/\epsilon$ , where  $\eta$  is the viscosity of the solvent,  $\mu$  is the electrophoretic mobility, and  $\epsilon$  is its dielectric constant. Hydrodynamic diameters ( $D_H$ ) were calculated from the diffusion coefficient ( $D$ ), using the Stokes–Einstein equation:  $D_H = kT/3\pi\eta D$ , where  $k$  is the Boltzmann constant and  $T$  the absolute temperature. Aliquots of the vesicle suspension were added to the appropriate amount of peptide stock solution in Tris-HCl buffer (pH 7.5) in 1.5 mL plastic vials, so that the final lipid concentration was 100  $\mu$ M. Each peptide/vesicle suspension, with P:L ratios ranging from 0:100 to 9:100, was equilibrated for 30 min at 25  $^\circ$ C before being measured. Next they were transferred to disposable cuvettes for size evaluation and, afterward, for  $\zeta$  potential measurements to a DTS1060 cell, which is equipped with golden electrodes (Malvern Instruments).

## RESULTS

**MP-1 Compromises Human Leukemic T Cell Survival Targeting Its Membrane.** The antitumor action of MP-1 has been established in different cell lines, including prostate and bladder cells. Those studies suggest a mechanism that involves interaction with the lipid membrane.<sup>9</sup> Via comparison with healthy peripheral lymphocytes, we tested whether MP-1 at different concentrations can selectively affect the membrane integrity of Jurkat cells, a human leukemic T-lymphocyte cell line. We first investigated if the effects of MP-1 on cell viability are determined by necrosis or by DNA fragmentation. In both experiments, the cell cultures were incubated with propidium iodide, a highly water soluble fluorescent compound, which cannot pass through intact cell membranes. For DNA fragmentation analysis, Triton X-100 was also added to the incubation plates to permeabilize the cell membranes and allow for incorporation of the dye into the cell and further binding to DNA bases.

Panels A and B of Figure 1 show representative histograms of MP-1 treatment at different concentrations for experiments examining membrane integrity and DNA fragmentation, respectively. From 25  $\mu$ M, MP-1 causes a progressive decrease in the level of Jurkat cells with intact membranes. At 50  $\mu$ M, only 40% of the cells are intact (Figure 1C). Interestingly, the membrane integrity of primary lymphocytes showed some alteration above 75  $\mu$ M MP-1. In addition, DNA fragmentation was not observed at any MP-1 concentration in Jurkat or primary lymphocyte cells (Figure 1B,D). These results indicate that MP-1 is more toxic to the leukemic cells than to normal lymphocytes.

**MP-1 Forms Porelike Structures in Planar Lipid Bilayers.** The effect on the membrane integrity of Jurkat cells suggests that MP-1 can form porelike structures on phospholipid membranes. To test this hypothesis, we first added MP-1 to uncharged planar lipid bilayers. Electrical measurements on bilayers provide a method for evaluating the increase in conductance due to the formation of pore structures at low peptide concentrations, at which unitary events are expected to occur. Figure 2A shows stable and continuous recordings of the pore activity induced by MP-1. The activity exhibited rapid transitions between multiple levels and was

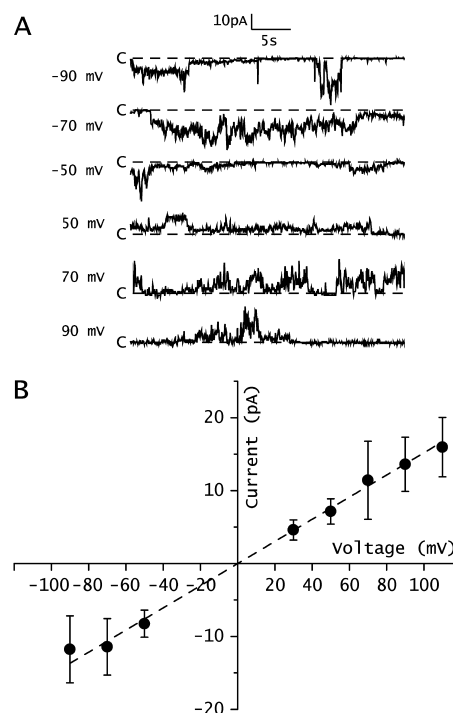


**Figure 2.** MP-1 pore-forming activity. (A) Representative single-channel current traces under steady-state conditions in zwitterionic DPhPC membranes with a membrane potential of  $-70$  mV. Currents were sampled at 200 Hz, filtered at 1 kHz, digitized, and off line low-pass filtered at 5 Hz. MP-1 was added to cis side of the membrane at a final concentration of 0.20  $\mu$ M. C denotes the closed conductive level. (B) Voltage–current relationship for the open-state pore of MP-1 pore-forming activity represented in panel A.

maintained for long periods of time. Figure 2B shows that the voltage–current relationship for the open state is linear. The porelike structure of MP-1 presents a predominant conductive state around 120 pS ( $n = 6$ ). However, MP-1 steep pore activity spikes were frequently observed with conductive levels up to 400 pS.

To test whether the lipid membrane composition affects MP-1 pore activity, we examined the interaction of MP-1 with membranes enriched in anionic lipids, sphingolipids or sterols. As depicted in Figure 3A, multilevel pore activity is characteristic of interaction of MP-1 with all compositions of bilayers tested. Eventually, some records of very small numbers of events showed well-defined pore transition events with anionic bilayers (data not shown). Figure 3A shows that there are preferred ionic amplitudes in bilayers of PC, PCPS, and PCCL. Some steep spikes can also be detected with PCCol, PCColSPH, and PCCL. These findings demonstrate that MP-1 pore activity does not require the presence of anionic lipids. Also, the presence of cholesterol at 20% of the total lipid composition significantly decreases the magnitude of the conductive events (Table 1), suggesting that the fluidity of the bilayers may have an important influence.

Moreover, we found that conductances in PC and in PCPS bilayers are undistinguishable and that the conductance observed in PCColSPH is slightly higher than that of PCCol (Figure 3 and Table 1). These unexpected findings can also be attributed to differences in bilayer fluidity (PC vs PCPS) and the domain formation characteristics of the cholesterol-containing membranes. If the fluid state of 100% PC bilayers should account for the intense MP-1 pore activity and in less

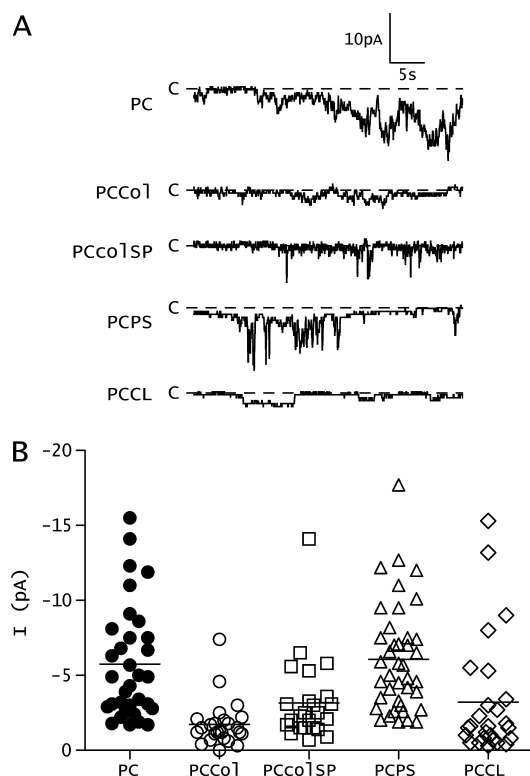


**Figure 3.** Effect of membrane composition on MP-1 pore-forming activity. (A) Representative single-channel current traces under steady-state conditions in membranes with different compositions. The membrane potential was set at  $-70$  mV for all membranes, except DPhPCColSPH, for which it was set at  $-90$  mV. Currents were sampled at 200 Hz, filtered at 1 kHz, digitized, and off line low-pass filtered at 5 Hz. MP-1 was added to the cis side of membrane at a final concentration of  $0.15$ – $0.30$   $\mu$ M. C denotes the closed conductive level. (B) Ionic current distribution of MP-1 pore-forming activity according to membrane phospholipid composition. Average current values for each bilayer are  $5.8 \pm 0.7$  pA for PC,  $1.7 \pm 0.3$  pA for PCCol,  $3.2 \pm 0.6$  pA for PCColSPH,  $6.1 \pm 0.6$  pA for PCPS, and  $3.2 \pm 0.8$  pA for PCCL.

fluid bilayers like PCPS (brain PS  $T_m$  is around  $0$ – $15$   $^{\circ}$ C) the level of poration should be reduced, the electrostatic interactions with the PS headgroup provided an increased level of binding (Table 1) and may compensate for the decrease in fluidity. The same effect cannot be seen in PCCL. Although the  $T_m$  of bovine heart CL is below  $-20$   $^{\circ}$ C, because of two points of unsaturation in each acyl chain, the characteristics of its headgroup region enhance membrane rigidity.<sup>20</sup> Membrane conductance is higher in PCPS than in PCCL probably as a

consequence of the higher membrane fluidity of PCPS, more favorable electrostatic interactions, or both. In PCColSPH bilayers, the formation of Ld domains enriched in PC could account for the increased conductance when compared to that of PCCol bilayers, although the difference in applied potential may also account for the difference in conductance.

**Binding of MP-1 to Lipid Bilayers.** The fluorescence blue shift and emission intensity data indicate changes in the polarity of the solvent environment around the Trp residue.<sup>21</sup> To quantitatively evaluate the binding of MP-1 on LUVs with different compositions, the Trp emission spectra were obtained in the absence and presence of increasing lipid concentrations. Figure 4A shows a representative set of spectra obtained for MP-1 in PC vesicles. The wavelength of maximal emission was 347 nm in the absence of LUVs, indicative of a polar environment for the Trp residue. Upon addition of LUVs, the fluorescence emission of MP-1 in PC vesicles was markedly shifted to lower wavelengths (blue shift) with higher intensities. Figure 4B shows that interaction of LUVs with MP-1 resulted in blue shifts, the extent of which was a function of the L:P molar ratio, that depend on the lipid composition of vesicles. The change in  $\lambda_{max}$  is greater in the presence of anionic vesicles, followed by the 100% PC vesicle, and strongly reduced in the vesicles containing cholesterol. These  $\lambda_{max}$  changes are indicative of a more hydrophobic environment around the Trp residue in anionic bilayers, reflecting affinities higher than those of zwitterionic bilayers.

The values for  $\Delta\lambda_{max}$  leveled off at an L:P ratio of  $\sim 10$  for the anionic vesicles, at an L:P ratio of  $\sim 70$  for PC LUVs, and at an L:P ratio of  $\sim 100$  for cholesterol-containing LUVs. We observed steeper and greater blue shifts in anionic bilayers and smoother and smaller shifts in LUVs containing cholesterol. Upon comparison of these data with those obtained for MP-1 in SDS micelles, which showed a more pronounced  $\Delta\lambda_{max}$ ,<sup>8</sup> the Trp residue in PCPS and PCCL vesicles seems to be located at the interface of the polar region, beneath the headgroup region.

**Assessing the Trp Environment.** The environment around Trp residues can be different in polarity and/or anisotropy levels. Characteristics of the environment around the peptide bound to LUVs can be assessed by Trp fluorescence emission anisotropy ( $r$ ) and by the acrylamide quenching of the emission spectra. The quantitative analysis of these data allows for the determination of the affinities of the peptide ( $K_p$ ) for the different vesicle compositions and for the calculation of the Stern–Volmer constants ( $K_{SV}$ ). The steady-state anisotropy measurement reveals the mobility of the fluorescent residue,<sup>17</sup> Trp, and is considered a sensitive

**Table 1.** MP-1 Concentrations in Planar Bilayers, Average Conductances Observed at an Applied Potential of  $-70$  mV, Except for PCColSPH That Was Observed at  $-90$  mV, Partition Coefficients ( $K_p$ ) Calculated from Trp Anisotropy Experiments According to Matos et al.,<sup>19</sup> Molar Fractions of Bound Peptide Molecules ( $X_B$ ), and Stern–Volmer Constants ( $K_{SV}$ )<sup>a</sup>

	[MP-1] ( $\mu$ M)	average conductance (pS)	$K_p$ ( $\times 10^3$ M $^{-1}$ )	$X_B$	$K_{SV}$ (M $^{-1}$ )
Tris buffer	–	–	–	–	$13.5 \pm 0.2^b$
PCCL	0.29	$46 \pm 11$	$26 \pm 3$	0.68	$5.2 \pm 0.1$
PCPS	0.18	$87 \pm 9$	$11.1 \pm 0.8$	0.48	$3.96 \pm 0.08$
PC	0.20	$83 \pm 10$	$5.2 \pm 0.2$	0.28	$7.1 \pm 0.2$
PCCol	0.30	$24 \pm 4$	$1.6 \pm 0.1$	0.11	$8.00 \pm 0.09$
PCColSPH	0.15	$36 \pm 7$	$1.24 \pm 0.08$	0.09	$10.09 \pm 0.02$

<sup>a</sup>The minimal  $R^2$  was 0.95 for partition coefficients and  $>0.99$  for Stern–Volmer constants. <sup>b</sup>Exponential fit.

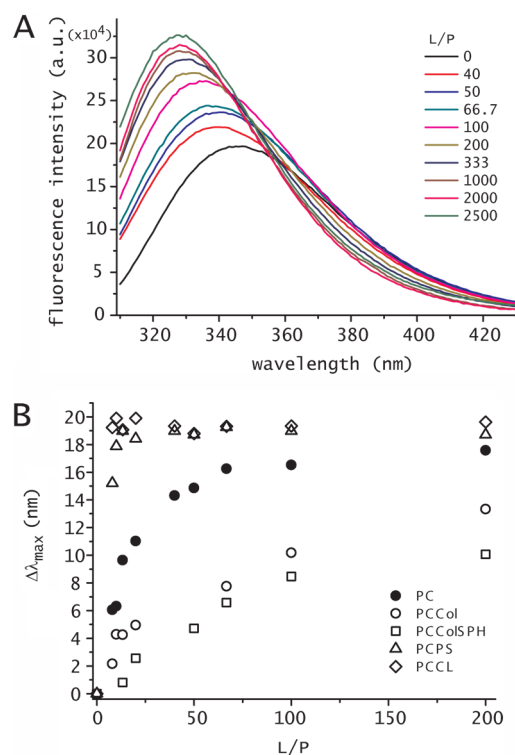


**Figure 4.** Lipid-induced changes in MP-1 tryptophan fluorescence. (A) Representative fluorescence spectra of MP-1 in the absence and presence of increasing concentrations of PC LUVs. L:P represents the lipid:peptide molar ratio. Spectra follow the increase in lipid concentration (from bottom to top). (B) Blue shift ( $\Delta\lambda_{\text{max}}$ ) for Trp in the wavelength of maximal emission in the presence of LUVs of different compositions as a function of lipid:peptide molar ratio. The MP-1 concentration in all experiments was  $5 \mu\text{M}$ , in the presence of  $10 \text{ mM}$  Tris-HCl buffer containing  $0.1 \text{ mM}$  EDTA and  $150 \text{ mM}$  NaCl (pH 7.5). The temperature was kept at  $25^\circ\text{C}$  with a circulating bath. The excitation wavelength was  $280 \text{ nm}$ . Emission and excitation polarizers were set and oriented at  $0^\circ$  and  $90^\circ$ , respectively, relative to the vertical.

technique for determining the association of fluorescent molecules with bilayers.<sup>21</sup>

Figure 5A shows the enhancement of anisotropy values upon binding of MP-1 to increasing concentrations of lipids with different LUV compositions. In the absence of lipids,  $r$  values of  $\sim 0.01$  were found, correlated with the rapid Brownian rotational diffusion of the peptide in aqueous solution. In the presence of vesicles,  $r$  values significantly increase, showing that Trp has limited diffusion in membrane mimetic environments. The highest  $r$  values were found with PCPS vesicles. They indicate that MP-1 mobility is more restricted in this membrane and notably different from the interactions with the other bilayers. The anisotropy versus lipid concentration plots were fit with the equation proposed by Matos et al.<sup>19</sup> The values obtained for the partition coefficients appear to correlate with the degree of negative charge in the membrane: PCCL > PCPS > electrically neutral vesicles (Table 1). Also, it was observed from the blue shift data that the peptide partitions more to the anionic than to the zwitterionic vesicles. The lowest affinities were those observed with PCCol and PCColSPH.

Partition coefficients on the order of  $10^3$  have been determined for several antimicrobial peptides,<sup>22</sup> including other mastoparans.<sup>23–25</sup> In this work,  $K_p$  values in anionic

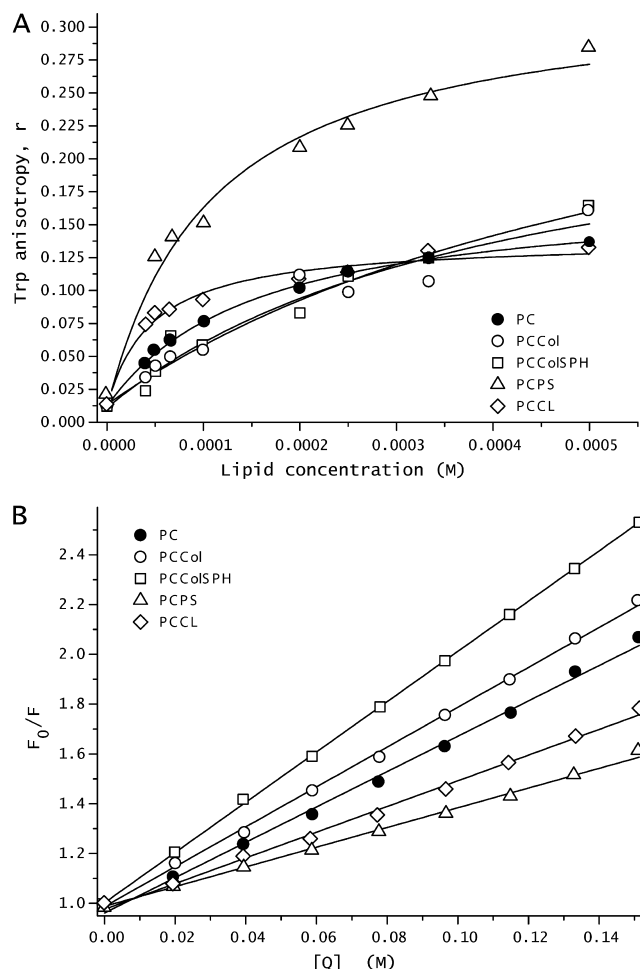


**Figure 5.** Assessing the Trp environment. (A) Trp fluorescence anisotropy in the presence of increasing concentrations of LUVs with different compositions. (B) Stern–Volmer plots for the quenching of Trp fluorescence emission by acrylamide in the presence of  $500 \mu\text{M}$  LUVs. Stern–Volmer constants were obtained from fitting with the equation  $F_0/F = 1 + K_{\text{SV}}(Q)$  for the curves obtained in the presence of vesicles. The excitation wavelength was at  $280 \text{ nm}$ . Emission and excitation polarizers were set and oriented at  $0^\circ$  and  $90^\circ$ , respectively, relative to the vertical. The MP-1 concentration was  $5 \mu\text{M}$  in Tris-HCl buffer containing  $0.1 \text{ mM}$  EDTA and  $150 \text{ mM}$  NaCl (pH 7.5). The temperature was kept at  $25^\circ\text{C}$ .

vesicles were found to be at least 1 order of magnitude higher than those in vesicles containing cholesterol.

Upon interaction with different bilayers, peptides exhibit variable levels of Trp fluorescence emission reflecting their exposure to a more or less hydrophilic environment. Acrylamide is a water-soluble collisional quencher of Trp fluorescence emission, whose interaction with bilayers is considered insignificant.<sup>26</sup> Titrating a solution of peptides with acrylamide in the absence and presence of LUVs, and analyzing maximal intensity data, according to the Stern–Volmer equation for collisional quenching, provides a measure of peptide binding through the Stern–Volmer constant ( $K_{\text{SV}}$ ). The higher the  $K_{\text{SV}}$ , the more exposed the peptide (Trp) is to the aqueous solvent. Figure 5B presents Stern–Volmer plots of the interaction of MP-1 with LUVs with different compositions. In relation to PC vesicles, it shows that the addition of cholesterol and sphingomyelin further impairs the penetration of the Trp residue into the more hydrophobic regions of the



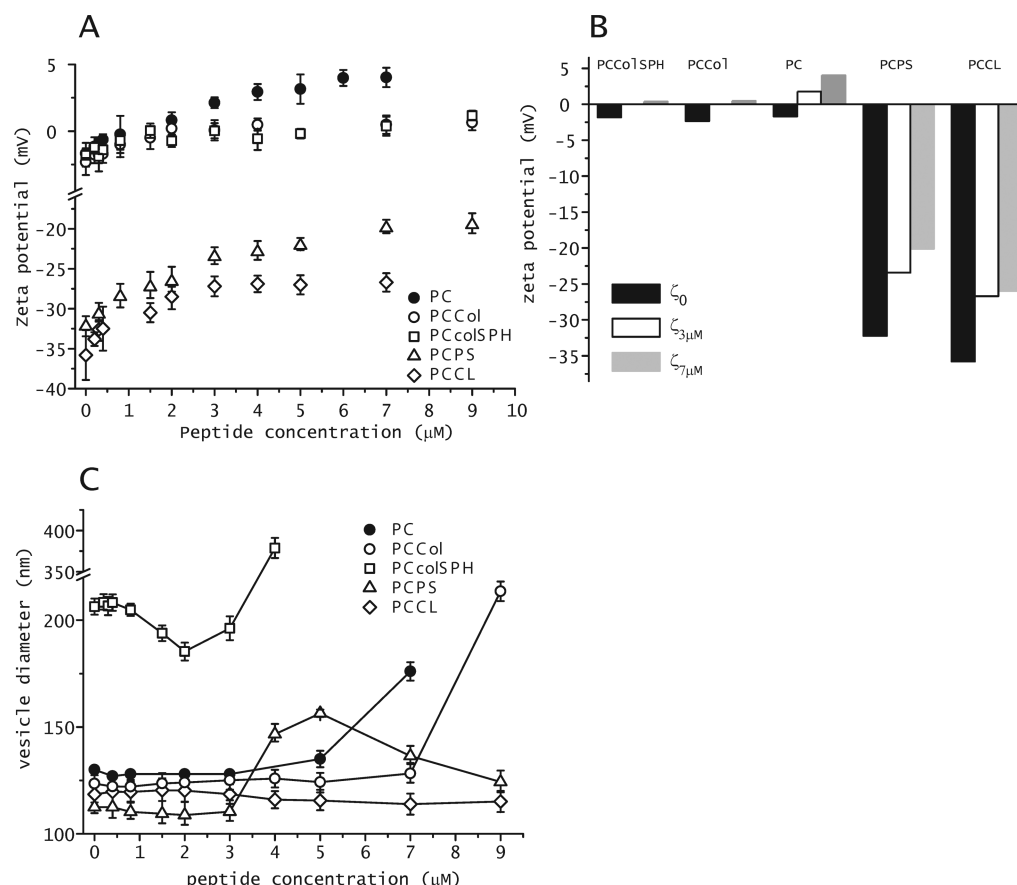


**Figure 6.** Effect of MP-1 concentration on the  $\zeta$  potential of membranes with different compositions. (A)  $\zeta$  potentials were measured in LUVs with different compositions in the presence of increasing concentrations of MP-1. The measurements were taken after equilibration for 30 min at 25 °C. (B)  $\zeta$  potentials of LUVs with different compositions in the absence ( $\zeta_0$ ) and presence of 3  $\mu\text{M}$  MP-1 ( $\zeta_{3\mu\text{M}}$ ) and 7  $\mu\text{M}$  MP-1 ( $\zeta_{7\mu\text{M}}$ ). In the presence of zwitterionic bilayers, diagrams display the potential reversal. (C) MP-1 size effects on LUVs with different compositions. The variation in the apparent vesicle diameter is shown as a function of peptide concentration, as determined from DLS, after equilibration for 1 h at 25 °C. The LUV concentration was 100  $\mu\text{M}$  in 10 mM Tris-HCl buffer containing 0.1 mM EDTA and 150 mM NaCl (pH 7.5).

membrane, while the anionic phospholipids promote a deeper insertion. Table 1 presents the Stern–Volmer constants for collisional quenching, calculated for each membrane in comparison to the  $K_{SV}$  value obtained for MP-1 in Tris buffer. These constants show that the bilayers partially protect Trp residues from the quencher, with PCPS vesicles showing the smaller constant or the most protected and PCColSPH the most exposed environment. It must be pointed out that the plot for MP-1 in Tris buffer deviates from linearity, reflecting static quenching, which is due to the presence of the quencher, acrylamide, in the vicinity of the Trp residue being excited. Accordingly, the respective  $K_{SV}$  was calculated by applying  $F_0/F = 1 + K_{SV}(Q) \exp[V(Q)]$ , where  $V$  is a constant for static quenching.<sup>27</sup> All the other  $K_{SV}$  values were checked for static quenching, and the results were the same as those for collisional quenching.

There is a negative correlation between  $K_p$  and  $K_{SV}$  values, except for the interaction with PCCL. According to Lewis and McElhaney,<sup>20</sup> effects of polar headgroups are interdependent of variations in the fatty acyl group. In the liquid crystalline state, CL headgroup flexibility and reorientational mobility are hindered. There is also a tendency to form inverted nonlamellar phases when the negative charges of phosphate groups are screened by ionic effects, including peptides. As a consequence of CL structural features in the headgroup area, cohesive interactions are enhanced in the hydrocarbon chain region and

at the polar–apolar interface that makes CL contribute to higher rigidity in the membranes. Another consequence pointed out is the obstruction of steric self-shielding of phosphate groups by interfacial glycerol, which results in more accessible interactions with the solvent for CL.

**Adsorption of MP-1 onto the Surface of LUVs.** To evaluate the accumulation of MP-1 on the surface of LUVs with different compositions,  $\zeta$  potential measurements were conducted in the absence and presence of MP-1 at several concentrations (Figure 6A). An increase in the  $\zeta$  potential was observed up to 2.0–3.0  $\mu\text{M}$  added peptide in all types of membranes. It then almost levels off at the higher peptide concentrations. These data also show that binding and accumulation of peptides at the surface of vesicles are strongly influenced by the presence of anionic phospholipids and that the presence of cholesterol hinders further binding of peptide molecules after the achievement of the potential reversal. Values of the  $\zeta$  potential for the vesicles, in the absence ( $\zeta_0$ ) and presence of 3  $\mu\text{M}$  MP-1 ( $\zeta_{3\mu\text{M}}$ ) and 7  $\mu\text{M}$  MP-1 ( $\zeta_{7\mu\text{M}}$ ), are shown in Figure 6B. These data emphasize the role of cholesterol in attenuating MP-1 binding and of the anionic lipids in strengthening peptide binding in relation to that of PC vesicles. CL with four acyl chains and two phosphates in the headgroup region does not show double anionic charge at the same molar concentration as PS, as denoted by their respective  $\zeta_0$  values of −35.8 and −32.2 mV for PCCL and PCPS,



respectively. The  $\zeta_0$  values indicate that under this experimental condition the CL net charge is  $-1.1$ , corroborating the value of  $-1.2$  found by Haines and Dencher.<sup>28</sup> At  $3 \mu\text{M}$  peptide, the vesicle charge densities of PCCL and PCPS were reduced by approximately 24 and 27%, respectively, while at  $7 \mu\text{M}$ , the reductions were 25 and 38%, respectively.

With the exception of PCCL bilayers, the adsorption of peptides at concentrations above  $3 \mu\text{M}$  causes some vesicles to expand depending on the lipid composition (Figure 6C). Although it was also observed that vesicles are leaky with respect to an entrapped probe at this concentration of MP-1,<sup>8</sup> the vesicle size distribution histograms are monomodal. This behavior could be partially attributed to the adsorption of the peptides and also to vesicle hemifusion or aggregation, though with other peptides these modifications were observed at lower peptide:lipid ratios.<sup>29,30</sup>

An increase in vesicle size followed by a decrease in size at higher P:L ratios induced by MP-1 in PCPS suggests that morphological changes may take place, favored by electrostatic interactions of the positively and negatively charged residues in MP-1 with multiple charge sites present on the PS headgroup.<sup>31</sup> At higher P:L ratios, a peptide/lipid aggregate may form in PCPS that would be neither necessary nor possible for the PCCL bilayer because of its higher and exclusively anionic charge, or its higher bending modulus. We have previously observed that mastoparan peptides, including MP-1, can form denser regions on the surface of giant vesicles (GUVs). These regions are similar to lumps and probably consist of by an aggregation of peptides and lipids.<sup>32</sup> These lumps did not seem to be static events but one intermediate step, sometimes quite long, between the lytic step and the final disintegration of the vesicle. Similar segregated regions were also observed with other peptides.<sup>33–35</sup>

## DISCUSSION

The mechanism for the selective toxicity of MP-1 to tumor cells is not well established. Wang et al.<sup>3</sup> showed that tumor cell membranes are disrupted by MP-1, which they attributed to the probable formation of a pore. We found that MP-1 is toxic to leukemic lymphocytes at concentrations above  $25 \mu\text{M}$  but may not compromise normal lymphocytes until  $75 \mu\text{M}$ . Our flow cytometer experiments revealed that the toxic effect involves a loss of membrane integrity and, indeed, required no DNA fragmentation. We thus hypothesized that MP-1 would disrupt lipid membranes by forming porelike structures. We obtained direct experimental evidence to support this hypothesis from planar lipid bilayers, with MP-1 showing at submicromolar concentrations intense pore activity in either anionic (PCPS) or zwitterionic (PC) bilayers.

Even though at first glance our planar lipid bilayer experiments in PC and PCPS can show the ability of MP-1 to form porelike structures, they cannot completely explain the mechanism of selectivity. We propose that the selectivity of MP-1 may be related to several differences in lipid composition between leukemic cells and normal lymphocytes. Healthy lymphocytes have lower levels of anionic phospholipids and significantly higher levels of cholesterol and sphingomyelin than leukemic ones.<sup>36</sup> Additionally, a significant decrease in the level of sphingomyelin is observed in the peripheral blood mononuclear cells of patients with acute leukemia.<sup>37</sup>

Upon comparison of the activity of MP-1 in planar lipid bilayers with different compositions (Figure 3 and Table 1), it can be observed that the peptide induced higher average

conductances in PC and PCPS bilayers than in PCCL and PCCol bilayers. The presence of cholesterol or cardiolipin in the membranes indeed drastically impairs pore formation. This is consistent with the observation that the presence of cholesterol or cardiolipin in membranes induces similar effects.<sup>8,38</sup> Furthermore, MP-1 activity in PCCol bilayers correlates well with the absence of hemolytic activity observed in rat red blood cells.<sup>6</sup> The low transmembrane currents recorded may suggest that the weakened electrostatic interactions between the membrane and the peptide, associated with the changes in fluidity attributed to cholesterol, impair the binding of MP-1 to the erythrocyte membrane.

From our planar lipid bilayer experiments, two major conclusions can be drawn. (i) The presence of the anionic lipid PS or cardiolipin in PC bilayers generates different behavior. While PS does not change the pore activity of MP-1, cardiolipin considerably reduces it. (ii) Compared with the presence of 100% PC, the presence of cholesterol in PC bilayers strongly prevents the pore activity of MP-1.

To understand the reasons why MP-1 does not induce similar porelike behavior in the anionic bilayers, we investigated the binding of MP-1 and its ability to accumulate and neutralize charged membranes. Trp emission spectra show that the membrane association of MP-1 was enhanced by the presence of negatively charged lipids. Although more specific techniques are required to confirm the depth of burial of the peptide, the fact that  $\Delta\lambda_{\text{max}}$  is close in both anionic LUVs confirms that the polarity of the environment around Trp residues is similar and may suggest an equivalent penetration depth of MP-1 (Figure 4B). The set of Trp interactions with polar groups of the environment may be different in their relative composition (hydroxyl groups and water molecules) in PCPS and PCCL, but they sum up as the same blue shift value. The partition coefficients obtained from Trp fluorescence anisotropy in the different bilayers (Table 1) confirm that MP-1 binds preferentially to anionic bilayers. Considering PCCL, it was demonstrated that lipids with smaller headgroups or with a greater acyl chain–headgroup differential, like cardiolipin, have more space to accommodate the peptide adsorption. Considering PCPS, although it presents coefficients smaller than those of PCCL, the highest value of anisotropy observed demonstrates that Trp residues are considerably more restricted in their diffusion than in the other anionic and zwitterionic bilayers.<sup>18,39</sup> Additionally, Stern–Volmer constants show that in PCPS LUVs, Trp is buried in an environment less accessible to the quencher than in PCCL, which might reflect the different curvature strains and the different electrostatic interactions in the headgroup region. The greater the  $K_p$ , the lower the  $K_{SV}$  (except for PCCL data). In other words, greater partition coefficients are correlated with MP-1 molecules less exposed to the aqueous environment (Table 1). In CL-containing vesicles, an increased number of peptide molecules are bound, but CL headgroup characteristics expose them more to the solvent and restrict them less in their mobility than PCPS. In this bilayer, the multiple sites for charged residue neutralization provide reduced peptide mobility. Differences in bilayer fluidity may account for the reduced pore activity of MP-1 observed in PCCL in relation to PCPS.

We have also shown that the presence of cholesterol drastically weakened the interaction of MP-1 with zwitterionic LUVs, denoted by reduced partition coefficients and increased  $K_{SV}$  constants. The rather small increase in  $\zeta$  upon addition of MP-1 to PCCol vesicles confirms the poor binding, and the

flatness of the  $\zeta$  potential curves suggests that  $<1 \mu\text{M}$  peptide is enough to hinder further binding. Those results are in accordance with the fact that cholesterol affects the fluidity and the dipole potential of phospholipid membranes,<sup>40</sup> inducing the ordering of the acyl chain region.<sup>41</sup> In this way, the attenuation of the porelike activity of PCCol bilayers can be correlated with the increase in the compressibility and bending moduli, hampering lytic activity.

In summary, our study shows that MP-1 targets the cell membrane of leukemic T-lymphocyte cells, inducing necrosis at a dose much smaller than that needed to induce necrosis in normal lymphocytes. The mechanism of this process may be attributable to the reduced binding of MP-1 to membranes containing cholesterol and sphingomyelin, which results in decreased pore activity. Cationic antimicrobial peptides that also exhibit tumoricidal activity can be considered a promising group of new leading compounds, because of their increased toxicity against tumorigenic cells versus normal cells. Selective targeting of membranes also provides the ability to kill cells that become resistant to other agents.

## AUTHOR INFORMATION

### Corresponding Author

\*M.P.d.S.C.: Department of Chemistry and Environmental Sciences, IBILCE, UNESP, R. Cristóvão Colombo, 2265, 15054-000 São José do Rio Preto, SP, Brazil (present address); telephone, 55-17-32212289; fax, 55-17-32212356; e-mail, cabrera.marcia@gmail.com. M.A.-M.: Department of Biophysics, UNIFESP, R. Botucatu, 862-7° andar, 04023-062 São Paulo, SP, Brazil; telephone, 55-11-5576-4555, ext. 214; fax, 55-11-5571-5780; e-mail, arcisio.miranda@unifesp.br.

### Funding

This work was supported in part by grants from the Council for Scientific and Technological Development (CNPq) [M.P.d.S.C. (postdoc 154550/2006-0), M.A.-M. (477780/2010-5), J.P. (301064/2004-0), and J.R.N. (306821/2009-5)] and Fundação de Amparo à Pesquisa do Estado de São Paulo (FAPESP) [M.S.P. and J.R.N. (06/57122-7), J.R.N. (07/03657-0), M.A.-M. (2010/52077-9), and M.P.d.S.C. (2010/11823-0)].

### Notes

The authors declare no competing financial interest.

## ACKNOWLEDGMENTS

We are thankful to Prof. Dr. Marcio F. Colombo for the use of the spectrofluorometer. We also acknowledge the assistance of Mr. Adi Kelvianto Harun from the Centre for Molecular Nanoscience at the University of Leeds (Leeds, U.K.) and Miss Deborah Capes from the Department of Neuroscience at the University of Wisconsin (Madison, WI) with the English.

## ABBREVIATIONS

MP-1, Polybia-MP1; BLM, planar bilayer lipid membrane; CL, cardiolipin;  $K_{ap}$ , apparent partition constant;  $K_p$ , intrinsic partition constant; LUVs, large unilamellar vesicles; PC, phosphatidylcholine; PCCol, PC/cholesterol mixture; PCColSPH, PC/cholesterol/sphingomyelin mixture; L:P, lipid:peptide molar ratio; PS, 1,2-diacyl-*sn*-glycero-3-phospho-L-serine; SPH, sphingomyelin.

## REFERENCES

- (1) Palma, M. S. (2006) Insect venom peptides. In *The handbook of biologically active peptides* (Kastin, A. J., Ed.) Vol. 56, pp 409–416, Elsevier, Amsterdam.
- (2) Konno, K., Rangel, M., Oliveira, J. S., Dos Santos Cabrera, M. P., Fontana, R., Hirata, I. Y., Hide, I., Nakata, Y., Mori, K., Kawano, M., Fuchino, H., Sekita, S., and Ruggiero Neto, J. (2007) Decoralin, a novel linear cationic  $\alpha$ -helical peptide from the venom of the solitary eumenine wasp *Oreumenes decoratus*. *Peptides* 28, 2320–2327.
- (3) Wang, K. R., Zhang, B. Z., Zhang, W., Yan, J. X., Li, J., and Wang, R. (2008) Antitumor effects, cell selectivity and structure-activity relationship of a novel antimicrobial peptide Polybia-MPI. *Peptides* 29, 963–968.
- (4) Hirai, Y., Yasuhara, T., Yoshida, H., Nakajima, T., Fujino, M., and Kitada, C. (1979) A new mast cell degranulating peptide “mastoparan” in the venom of *Vespula lewisii*. *Chem. Pharm. Bull.* 27, 1942–1944.
- (5) Nakajima, T., Uzu, S., Wakamatsu, K., Saito, K., Miyazawa, T., Yasuhara, T., Tsukamoto, Y., and Fujino, M. (1986) Amphiphilic peptides in wasp venom. *Biopolymers* 25, 115–121.
- (6) De Souza, B. M., Mendes, M. A., Santos, L. D., Marques, M. R., Cesar, L. M., Almeida, R. N., Pagnocca, F. C., Konno, K., and Palma, M. S. (2005) Structural and functional characterization of two novel peptide toxins isolated from the venom of the social wasp *Polybia paulista*. *Peptides* 26, 2157–2164.
- (7) De Souza, B. M., da Silva, A. V., Resende, V. M., Arcuri, H. A., Dos Santos Cabrera, M. P., Ruggiero Neto, J., and Palma, M. S. (2009) Characterization of two novel polyfunctional mastoparan peptides from the venom of the social wasp *Polybia paulista*. *Peptides* 30, 1387–1395.
- (8) Dos Santos Cabrera, M. P., Costa, S. T., de Souza, B. M., Palma, M. S., Ruggiero, J. R., and Ruggiero Neto, J. (2008) Selectivity in the mechanism of action of antimicrobial mastoparan peptide Polybia-MP-1. *Eur. Biophys. J.* 37, 879–891.
- (9) Wang, K. R., Yan, J. X., Zhang, B. Z., Song, J. J., Jia, P. F., and Wang, R. (2009) Novel mode of action of Polybia-MPI, a novel antimicrobial peptide, in multi-drug resistant leukemic cells. *Cancer Lett.* 278, 65–72.
- (10) Zhang, W., Li, J., Liu, L. W., Wang, K. R., Song, J. J., Yan, J. X., Li, Z. Y., Zhang, B. Z., and Wang, R. (2010) A novel analog of antimicrobial peptide Polybia-MPI, with thioamide bond substitution, exhibits increased therapeutic efficacy against cancer and diminished toxicity in mice. *Peptides* 31, 1832–1838.
- (11) Boyum, A. (1968) Isolation of leucocytes from human blood. Further observations. Methylcellulose, dextran, and ficoll as erythrocyte aggregating agents. *Scand. J. Clin. Lab. Invest.* 97, 31–50.
- (12) Nicoletti, I., Migliorati, G., Pagliacci, M. C., Grignani, F., and Riccardi, C. (1991) A rapid and simple method for measuring thymocyte apoptosis by propidium iodide staining and flow cytometry. *J. Immunol. Methods* 139, 271–279.
- (13) Mueller, P., Rudin, H. T., Tien, T., and Wescott, W. C. (1963) Methods for the formation of single bimolecular lipid membranes in aqueous solutions. *J. Phys. Chem.* 67, 534–535.
- (14) Dos Santos Cabrera, M. P., Arcisio-Miranda, M., Da Costa, L. C., De Souza, B. M., Broggio Costa, S. T., Palma, M. S., Ruggiero Neto, J., and Procopio, J. (2009) Interactions of mast cell degranulating peptides with model membranes: A comparative biophysical study. *Arch. Biochem. Biophys.* 486, 1–11.
- (15) Chattopadhyay, A., Rawat, S. S., Greathouse, D. V., Kelkar, D. A., and Koepp, R. E., II (2008) Role of tryptophan residues in gramicidin channel organization and function. *Biophys. J.* 95, 166–175.
- (16) Ladokhin, A. S., Jayasinghe, S., and White, S. H. (2000) How to measure and analyze tryptophan fluorescence in membranes properly, and why bother? *Anal. Biochem.* 285, 235–245.
- (17) Lakowicz, J. R. (1999) *Principles of Fluorescence Spectroscopy*, Kluwer Academic/Plenum, New York.
- (18) Castanho, M. A., and Prieto, M. J. (1992) Fluorescence study of the macrolide pentaene antibiotic filipin in aqueous solution and in a model system of membranes. *Eur. J. Biochem.* 207, 125–134.

- (19) Matos, P. M., Franquelim, H. G., Castanho, M. A. R. B., and Santos, N. C. (2010) Quantitative assessment of peptide–lipid interactions. Ubiquitous fluorescence methodologies. *Biochim. Biophys. Acta* 1798, 1999–2012.
- (20) Kubo, S., Nemani, V. M., Chalkley, R. J., Anthony, M. D., Hattori, N., Mizuno, Y., Edwards, R. H., and Fortin, D. L. (2005) A combinatorial code for the interaction of  $\alpha$ -synuclein with membranes. *J. Biol. Chem.* 280, 31664–31672.
- (21) Marsh, D. (2009) Cholesterol-induced fluid membrane domains: A compendium of lipid-raft ternary phase diagrams. *Biochim. Biophys. Acta* 1788, 2114–2123.
- (22) Goñi, F. M., Alonso, A., Bagatolli, L. A., Brown, R. E., Marsh, D., Prieto, M., and Thewalt, J. L. (2008) Phase diagrams of lipid mixtures relevant to the study of membrane rafts. *Biochim. Biophys. Acta* 1781, 665–684.
- (23) Lewis, R. N., and McElhaney, R. N. (2009) The physicochemical properties of cardiolipin bilayers and cardiolipin-containing lipid membranes. *Biochim. Biophys. Acta* 1788, 2069–2079.
- (24) Sood, R., Domanov, Y., and Kinnunen, P. K. (2007) Fluorescent temporin B derivative and its binding to liposomes. *J. Fluoresc.* 17, 223–234.
- (25) Melo, M. N., Ferre, R., and Castanho, M. A. (2009) Antimicrobial peptides: Linking partition, activity and high membrane-bound concentrations. *Nat. Rev. Microbiol.* 7, 245–250.
- (26) Schwarz, G., and Reiter, R. (2001) Negative cooperativity and aggregation in biphasic binding of mastoparan X peptide to membranes with acidic lipids. *Biophys. Chem.* 90, 269–277.
- (27) Arbuzova, A., and Schwarz, G. (1999) Pore-forming action of mastoparan peptides on liposomes: A quantitative analysis. *Biochim. Biophys. Acta* 1420, 139–152.
- (28) Schwarz, G., and Blochmann, U. (1993) Association of the wasp venom peptide mastoparan with electrically neutral lipid vesicles. Salt effects on partitioning and conformational state. *FEBS Lett.* 318, 172–176.
- (29) De Kroon, A. I., Soekarjo, M. W., De Gier, J., and De Kruijff, B. (1990) The role of charge and hydrophobicity in peptide-lipid interaction: A comparative study based on tryptophan fluorescence measurements combined with the use of aqueous and hydrophobic quenchers. *Biochemistry* 29, 8229–8240.
- (30) Eftink, M. R., and Ghiron, C. A. (1976) Exposure of tryptophanyl residues in proteins. Quantitative determination by fluorescence quenching studies. *Biochemistry* 15, 672–680.
- (31) Haines, T. H., and Dencher, N. A. (2002) Cardiolipin: A proton trap for oxidative phosphorylation. *FEBS Lett.* 528, 35–39.
- (32) Cummings, J. E., and Vanderlick, T. K. (2007) Aggregation and hemi-fusion of anionic vesicles induced by the antimicrobial peptide cryptdin-4. *Biochim. Biophys. Acta* 1768, 1796–1804.
- (33) Sood, R., Domanov, Y., Pietiäinen, M., Kontinen, V. P., and Kinnunen, P. K. (2008) Binding of LL-37 to model biomembranes: Insight into target vs host cell recognition. *Biochim. Biophys. Acta* 1778, 983–996.
- (34) Fuller, N., Benatti, C. R., and Rand, R. P. (2003) Curvature and bending constants for phosphatidylserine-containing membranes. *Biophys. J.* 85, 1667–1674.
- (35) Dos Santos Cabrera, M. P., Alvares, D. S., Leite, N. B., De Souza, B. M., Palma, M. S., Riske, K. A., and Ruggiero Neto, J. (2011) New insight into the mechanism of action of wasp mastoparan peptides: Lytic activity and clustering observed with giant vesicles. *Langmuir* 27, 10805–10813.
- (36) Hasper, H. E., Kramer, N. E., Smith, J. L., Hillman, J. D., Zachariah, C., Kuipers, O. P., de Kruijff, B., and Breukink, E. (2006) An Alternative Bactericidal Mechanism of Action for Lantibiotic Peptides That Target Lipid II. *Science* 313, 1636–1637.
- (37) Zhao, H., Mattila, J. P., Holopainen, J. M., and Kinnunen, P. K. (2001) Comparison of the membrane association of two antimicrobial peptides, magainin 2 and indolicidin. *Biophys. J.* 81, 2979–2991.
- (38) Zhao, H., Tuominen, E. K., and Kinnunen, P. K. (2004) Formation of amyloid fibers triggered by phosphatidylserine-containing membranes. *Biochemistry* 43, 10302–10307.
- (39) Gottfried, E. L. (1967) Lipids of human leukocytes: Relation to cell type. *J. Lipid Res.* 8, 321–327.
- (40) Kuliszewicz-Janus, M., Tuz, M. A., Kielbiński, M., Jaźwiec, B., Niedoba, J., and Baczyński, S. (2009) <sup>31</sup>P MRS analysis of the phospholipid composition of the peripheral blood mononuclear cells (PBMC) and bone marrow mononuclear cells (BMMC) of patients with acute leukemia (AL). *Cell. Mol. Biol. Lett.* 14, 35–45.
- (41) Bechinger, B., and Lohner, K. (2006) Detergent-like actions of linear amphipathic cationic antimicrobial peptides. *Biochim. Biophys. Acta* 1758, 1529–1539.